SUBMERGED ARC WELD RESTORATION OF STEAM TURBINE ROTORS USING SPECIALIZED WELDING TECHNIQUES

by

Richard A. LaFave

Senior Welding Engineer

Elliott Company

Jeannette, Pennsylvania

Richard A. (Dick) LaFave graduated from Ohio State University with a B.S. degree in Welding Engineering (1968). He worked for several years with Jeffrey Mining Machinery Company, while finishing his M.B.A. degree also at Ohio State (1974). Mr. LaFave was employed by Westinghouse Electric Corporation at their Research and Development Center before joining the Elliott Company (1976).

Since joining Elliott, he has been involved in the designing of casings and baseplates, along with the welding or brazing of numerous rotating and stationary components used in compressors and turbines. He has a patent on a cold-extruded aluminum filler metal and has written papers on welding, brazing, and weld forming. He is a member of AWS where he has chaired a technical subcommittee and task groups on filler metals. He is currently First Vice Chairman of the AWS Committee on Filler Metal and a member or advisor to several AWS technical committees and ACIIW.

Mr. LaFave is a Registered Professional Engineer in the States of Ohio and Pennsylvania and a member director of the Pittsburgh Chapter of PSPE.

ABSTRACT

In the past 10 years, there have been significant gains made in the repair of steam turbine rotors by the use of welding. This has been the result of improvements in several areas dealing with materials, engineering analysis, nondestructive testing, and specialized welding techniques. Several papers have been written on the repair of LP rotors for central generating stations. A few have recently been written on repairs to HP rotors. There has been little written on the welded repair of mechanical drive steam turbine rotors.

The specialized welding techniques needed to perform submerged arc welding restoration of mechanical drive steam turbine rotors are highlighted. The advantages of welded repair and the engineering analysis necessary to make a reliable repair to a rotor are also addressed. Basically, two categories of welded repair are studied. One is the welded journal repair. The other is the complete replacement of a stage disc on a monoblock rotor forging by the use of welding. Mock up test assemblies are used, along with sample weld test assemblies, in order to try to duplicate the actual welding situation as much as possible. Both destructive and nondestructive testing is performed on these test assemblies to determine occurrence of any flaws, mechanical and electrical runout, chemical composition variations, hardness distributions, tensile and yield strength in different directions at room and elevated temperatures, fracture toughness, fracture appearance transition temperatures, stress rupture strength, and fatigue endurance limits. The results from these tests are discussed along with the pertinent engineering requirements that pertain in order to give the limits of welded repair. Plans for further testing are outlined, along with the conclusion that supports continued acceptance of submerged arc weld restoration of steam turbine rotors ensuring reliability of the weld metal and the heat affected zone of the turbine base material.

INTRODUCTION

Welded steam turbine rotor shafts were originally introduced 60 years ago due to limited supply of large monoblock forgings in Europe [1]. Over the last 20 years, there has been increased interest in steam turbine rotor shaft welding due to several significant developments.

- New steel making practices, such as vacuum treatment and basic electric furnace technology, permit steels to be made which are lower in sulphur, phosphorus, tin, antimony, arsenic, and lead [2].
- Welding fluxes and flux coverings are improved to control the introduction of hydrogen which may reduce weldability or assist cold cracking [3].
- Welding filler metals can be selected which will produce weld metal, which is often lower in $FATT_{50}$ than the rotor base metal and higher in fracture toughness [4, 5].
- Welding systems are available with improved control of parameters which affect the integrity of the weld being produced [6].
- Analytical engineering tools are available which allow engineers to more accurately evaluate stress and strain conditions at operating temperature and predict life extension through fracture and fatigue analysis [7].
- Nondestructive testing equipment and techniques are available that permit a more detailed examination of the damaged rotor shaft, as well as the final weld restored rotor shaft [8, 9].

This new interest has primarily been directed to the restoration of damaged rotor shafts. This damage can be transverse cracking due to high or low cycle fatigue. It can also be damage due to a mechanical failure or lost lubrication. Stress corrosion damage is a third major concern. This last type of damage usually occurs in highly stressed areas when the environment is such as to facilitate this type of pitting or cracking damage.

A philosophy of rotor shaft restoration using welding and recent fatigue, stress rupture, and creep data for submerged arc welded test assemblies are described herein. The data are derived from mechanical testing of both mock up test assemblies and weld sample test assemblies using materials that are normally specified in mechanical drive turbine rotors and in centrifugal compressor shafts.

PHILOSOPHY OF ROTOR SHAFT RESTORATION

Advantages of Welded Repair

Submerged arc welding restoration of rotor shafts offers certain advantages over complete replacement or mechanical fixes to damaged rotors. The economic advantage is one that is well understood upon merely looking at the delays and downtime and costs to completely replace a damaged rotor with a brand new one. It is not unusual to wait a year for a replacement forged rotor shaft and pay five to ten times more for it than would be paid for a weld repaired rotor delivered in less than a couple of months.

However, looking beyond this replacement option to the technical aspects of the fix option, a mechanical repair usually entails a sacrifice in equipment performance and may lead to future problems, if the mechanical fastening device loosens or creeps to the point where excessive vibration becomes evident and the equipment must be shut down again. A welded repair to a rotor is permanent with little chance of creep failure, provided the proper filler metal is used. Even chrome plating of journal areas in excessive thickness, usually greater than 0.030 in (0.8 mm), can flake off with time and introduce bearing failures. A welded journal repair to a rotor restores the bearing surfaces to original sound metal condition.

A welded repair to a rotor shaft involves complete coalescence of the metals and thus creates a full fusion, metal-to-metal bond without crevices. A complete integral disc replacement on a monoblock steam turbine rotor shaft forging, as shown in Figure 1, clearly depicts the extent to which weld restoration can be accomplished. The one concern that always arises is how have the base metal properties been altered after welding and postweld heat treatment and will these properties still be adequate to give continued reliable service for the equipment involved.

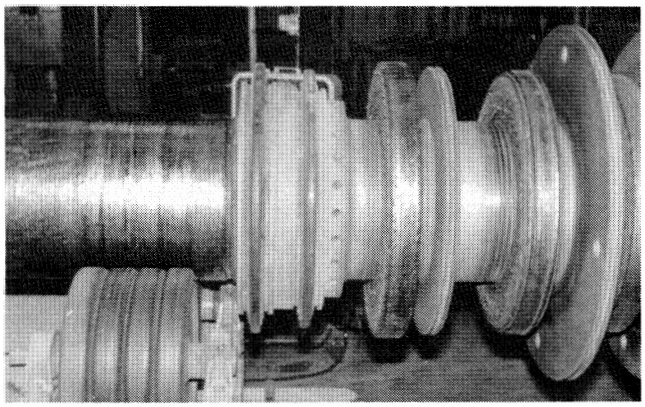

Figure 1. A Multiple Disc Buildup Repair of Steam Turbine Rotor Forging.

Heat Affected Zone

Primary concerns that arise with any weld repair of rotor shafts centers on the heat affected zone of the weld. This is the volume of base metal immediately adjacent to the fused weld metal, as shown in Figure 2. The heat affected zone (HAZ) does not resolidify as the weld metal does, but it is exposed to high temperatures approaching the melting point, which in steels is around 2500°F (1371°C). Therefore, the HAZ does not melt completely but does undergo transformation and hardening in the rotor steels. The mass quenching effect of the colder base metal surrounding the heat affected zone is significant and can result in higher hardness than those obtained in the normalized and tempered base metal, as shown in Figure 3.

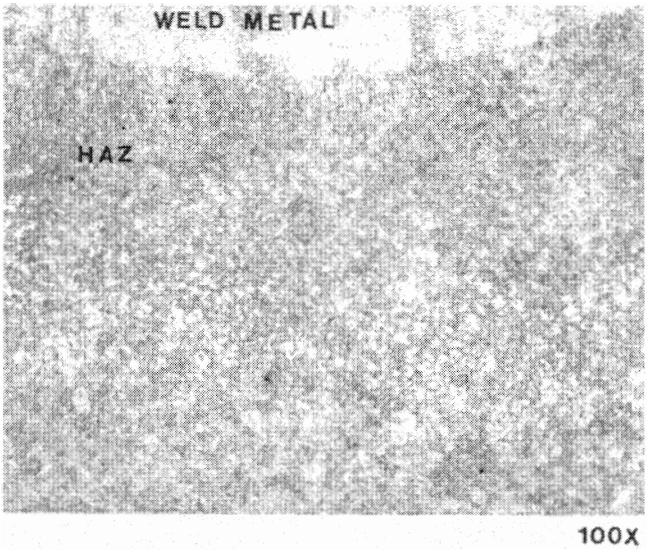

Figure 2. Microstructure of the Weld Metal and Heat Affected Zone.

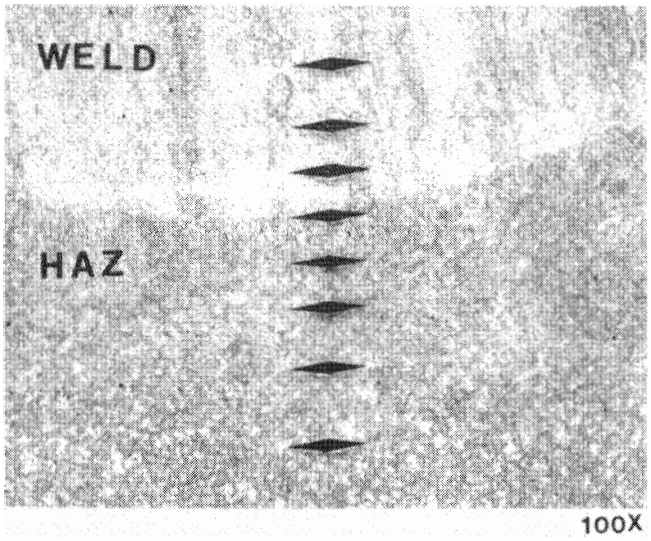

Figure 3. Hardness Indents in the Heat Affected Zone and Weld Metal.

To reduce the mass quenching effect, the temperature difference between the molten weld and the colder base metal can be reduced. This is done by preheating the base metal prior to welding. A soaking preheat of the base metal will reduce the temperature differences and reduce the temperature gradient. This will decrease the amount of self-quenching that may produce a less than desirable microstructure. The final result will be a microstructure in the HAZ which has good fracture toughness. Rotor steels are designed to be hardenable and require a higher than normal preheat temperature in order to preclude the formation of an undesirable microstructure.

Preheating can also prevent cold cracking. Cold cracking, or delayed underbead cracking or hydrogen-assisted cracking occurs when hydrogen atoms are rejected within the metal upon transformation from face-centered cubic to body-centered cubic crystalline lattice. The face-centered cubic crystal has a higher solubility limit for monatomic hydrogen than the body-centered cubic crys-

tal, as shown in Figure 4. This excess hydrogen becomes "trapped" in the solid metal and is thought to introduce lattice strain as it diffuses to certain preferred locations in the lattice. If the strain exceeds the threshold limit, it may result in dislocations within the lattice. If extreme external strains are also experienced due to restraint and process heating and cooling, these dislocations can "pileup" and microfissures can occur. These microfissures may then become cracks, given certain conditions, as shown in Figure 5.

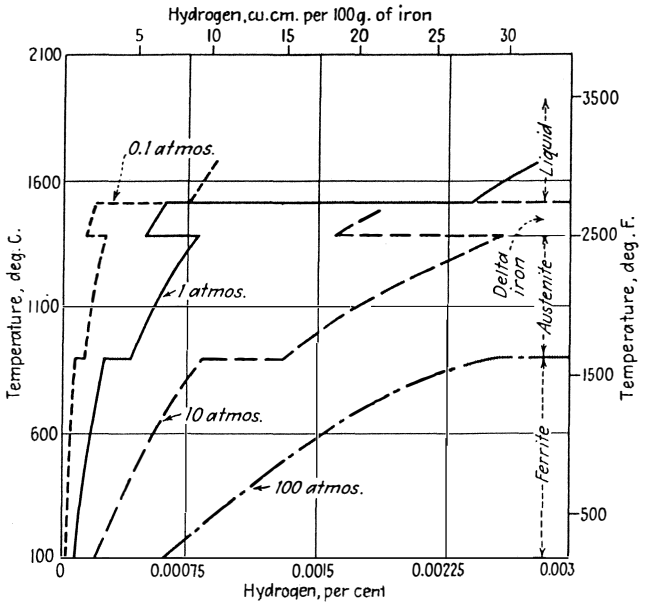

Figure 4. Solubility of Hydrogen in Iron [9].

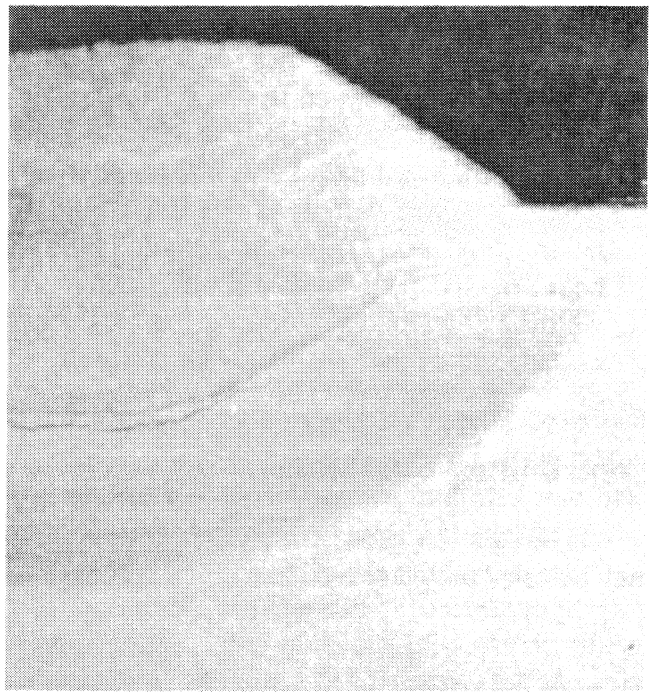

Figure 5. An Underbead Crack [10].

Preheating normally allows the metal to stretch more readily, since ductility of metals increases with increasing temperature. However, rotor steels, due to their design, tend to be creep resistant and do not show as much elongation increase as compared to some other steels. Preheating, in the case of rotor steels, does more to increase the diffusivity of hydrogen and allow some of these atoms to leave the steel, at which time they will form the diatomic gas. This outgasing will relieve the potential for excessive lattice strain. By increasing the temperature of the steel from 72°F (22°C) to 450°F (232°C), the diffusivity of hydrogen increases by 100 times, as shown in Figure 6. Therefore, preheating the steel, and holding the preheat for a sufficient length of time after completion of welding, can reduce the instance of delayed underbead cracking or cold cracking due to excessive hydrogen.

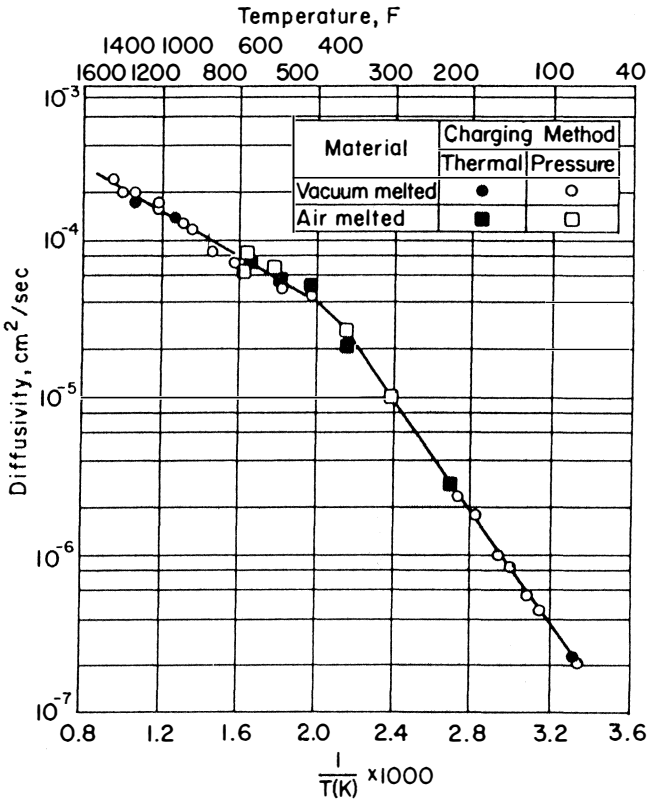

Figure 6. Diffusivity Coefficient of Hydrogen in Iron [9].

Fracture Analysis

Welds are never perfect. Neither are base metals. The objective is always to get an acceptable weld, which may not be a perfect weld. An acceptable weld is one in which there may be flaws, but they are not going to either fracture catastrophically when subjected to load nor grow to a size which could fracture catastrophically. This principle is well explained in literature concerning fracture mechanics [11, 12]. A generalized fracture analysis diagram as referenced by the Nil Ductility Temperature is shown in Figure 7.

Fracture mechanics and fracture analyses permit the determination of the acceptable flaw size that can be tolerated without fear of catastrophic failure. To reasonably predict the allowable flaw size, the following items should be known:

- The stress levels at various regions in the structure. Finite element analysis of both mechanical and thermal stresses is suggested.

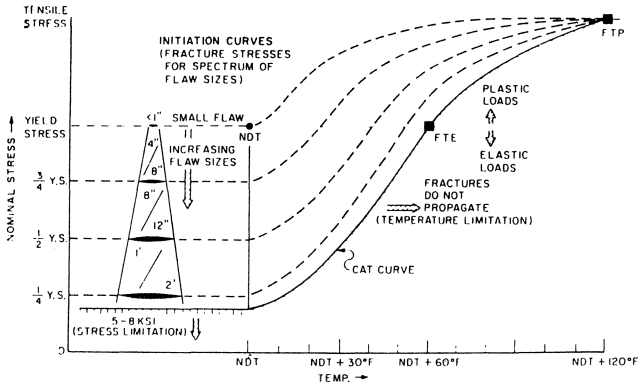

Generalized Fracture Analysis Diagram, as Referenced by the NDT Temperature, after Pellini and Puzak.[46] NDT = Nil Ductility Temperature; CAT = Crack Arrest Temperature; FTE = Fracture Transition, Elastic; and FTP = Fracture Transition, Plastic.

Figure 7. Fracture Analysis Diagram [11].

- Measurement of the degree of temper embrittlement that has occurred in the rotor material due to long term service at high temperature.
- Measurement of the effect of welding heat on fracture toughness of the actual rotor material or similar material.
- Measurement of the effect of postweld heat treatment on the recovery of toughness in the heat affected zone of the weld.

Fracture Appearance and Toughness

Fracture toughness in the rotor steels has been measured traditionally with the Charpy impact test specimen. These are the V-notched specimens per ASTM A370. Two acceptance criteria are usually used. One is the energy required to break the specimen at room temperature. The other acceptance criterion is the fracture appearance transition temperature or FATT. Steam turbine rotor material specifications require that a minimum average value of energy be attained in breaking the Charpy specimens at room temperature. Over the years, these values have increased. Therefore, rotors manufactured to the old ASTM A293 may not meet the higher toughness levels required in the new ASTM A470 Specification. Yet, there are exceptions, such as one rotor which is still in daily service nine years after it was weld repaired at the transition radius of the last wheel (L-0) towards the generator end. Preliminary testing of this rotor before repair welding gave room temperature average impact value of 31 ft-lbf (40J). This was well above the 12 ft-lbf (16J) minimum required.

The FATT measurement requires that Charpy specimens broken at the specified FATT temperature show at least 50 percent shear failure on the broken surface. In evaluating the degree of embrittlement that has taken place, the $FATT_{50}$ is measured by breaking several sets of Charpy specimens to find the testing temperature at which the fracture of the specimen is 50 percent ductile shear and 50 percent brittle cleavage. A relative comparison of the $FATT_{50}$ with the specified FATT provides a means of judging the degree of embrittlement. If the actual value is well below the specified value, then there should be very little embrittlement of the rotor. Shawville #4 rotor, after 22 years service, had a measured $FATT_{50}$ of 130°F (54°C), which is still 45°F (25°C) below the maximum specified FATT for A293-58T Class 3 rotor forging. The original equipment manufacturer had estimated that the value would be 220°F (104°C), according to Saha and Conway [4].

The vacuum treated Cr-Mo-V rotor steel per ASTM A470 Class 8 requires an FATT of no more than 250°F (121°C). This may seem high in comparison to other steam turbine rotor steels and certainly high in comparison to centrifugal compressor rotors. However, the application of the Cr-Mo-V rotor steels is usually at the highest temperature ranges for steam turbines. A compromise between good creep properties and good toughness must always be achieved. With the higher temperature materials, creep often gets more attention in the alloy design at the expense of some of the toughness.

In order to achieve a reliable weld restoration on a service turbine rotor, the existing material condition must be evaluated by the above techniques. Knowing the upper shelf impact values, one can make a reasonable estimate of the critical plain-strain stress-intensity factor, K_{Ic}, for the used rotor. The Rolfe-Novak-Barsom correlation [13, 14] of upper shelf Charpy values, CVN, with K_{Ic} numbers has been shown to be valid for most steam turbine rotor steels which operate at temperatures above the transition temperature range. This correlation is as follows:

$$\left[\frac{K_{IC}}{\sigma_{ys}}\right]^2 = \frac{5}{\sigma_{ys}}\left[CVN - \frac{\sigma_{ys}}{20}\right] \quad (1)$$

where

K_{IC} = critical plain-strain stress intensity factor, ksi $in^{1/2}$
σ_{ys} = yield strength, ksi
CVN = average upper shelf Charpy V notch energy value, ft-lbf

Engineered Approach

Evaluation is performed using material removed from the damaged area on the rotor that is being considered for weld repair. This material is cut apart from the rotor with sufficient coolant to prevent any extreme heating. Once the material has been removed, the following tests should be performed by a competent technician and engineer:

- Chemical analysis to verify chemical composition and identify any trace amounts of low melting point elements (Sn, Sb, As, and Pb).
- Charpy V notch impact testing for both room temperature and FATT results in order to judge the degree of embrittlement and estimate the K_{Ic} value.
- Mechanical strength properties in either radial or tangential or both directions, if possible.
- Metallographic analysis to determine type of microstructure present in the area to be welded and to look for any signs of degradation of the microstructure.

The results of these tests and the evaluations will usually give one a reasonable idea of whether a weld restoration is possible. Also, it can then be predicted with some certainty as to how well the restored rotor shaft will perform.

A sample weld test assembly can also be used to evaluate the actual base metal or, if that size of actual base metal is not available, then a piece of some similar base metal may have to be substituted. The welding of this test assembly should be done with parameters as close as possible to the actual welding parameters. The postweld heat treatment should also duplicate that which is intended to be used. The sample can then be tested to see how the welding and subsequent heat treatment affected the base metal in the heat affected zone of the test assembly.

Pragmatic Approach

The method so far described is the engineering method to assure a reliable repair and continued service without undue risk. If the risks of rotor failure are minimal and the repair is being done in a very low stress area not exposed to high temperatures, then a more pragmatic solution may be the best solution. This is commonly known as the "best effort—get it back in service quickly" approach. This approach can work, but it does depend on fortunate

outcomes. The only testing done in this pragmatic approach is nondestructive testing or examination with some simple chemical analysis.

The nondestructive testing consists of both crack detection and volumetric ultrasonic testing. Hardness testing using the resilience type testers can also be considered as nondestructive, because the slight indentation that results is usually insignificant, if left in an area other than the actual journal areas.

The key to any nondestructive testing done to detect flaws in the rotor or in the repair is to be able to detect a flaw size small enough to preclude missing a defect which could be harmful. With the pragmatic approach to restoration, conservative, intuitive limits of acceptable flaw size must often be used based on experience. Often the limit set is the capability of the NDT method. This would, for example, be a 1/16 in (1.6 mm) linear indication for crack detection and a 1/16 in (1.6 mm) diameter side drilled hole for ultrasonic testing. Investigation, documentation, and removal of any flaw exceeding these limits would be required. Fracture analysis and testing, on the other hand, would indicate that flaw sizes of three to four times these intuitive flaw sizes may be acceptable in regions of low stress for rotor steels with a K_{Ic} in excess of 100 ksi $in^{1/2}$(110MN $m^{-3/2}$). However, this fracture analysis can be well beyond the basic understanding of most NDT operators and many engineers and, therefore, is not readily applied when the pragmatic approach is used.

Crack Growth Behavior

The critical flaw size for dynamic loading is less than that for static loading due to fatigue crack growth behavior. A relationship was developed by Paris [15] to formulate fatigue crack growth rate, as follows:

$$da/dN = C(\Delta K)^n \quad (2)$$

where

da/dN = crack growth per cycle of loading, inch per cycle
ΔK = dynamic stress-intensity factor, ksi $in^{1/2}$
C = material constant
n = exponent

This equation is linear on a log-log plot of ΔK versus da/dN. When empirical data is plotted for martensitic steels, this equation is accurate for a range of rates from 10^{-4} to 10^{-5} in per cycle. Such a plot summary is shown in Figure 8. The conservative upper limit boundary for crack growth rate utilizes a material constant, C, equal to 0.66×10^{-8} and an exponent, n, equal to 2.25. This constant

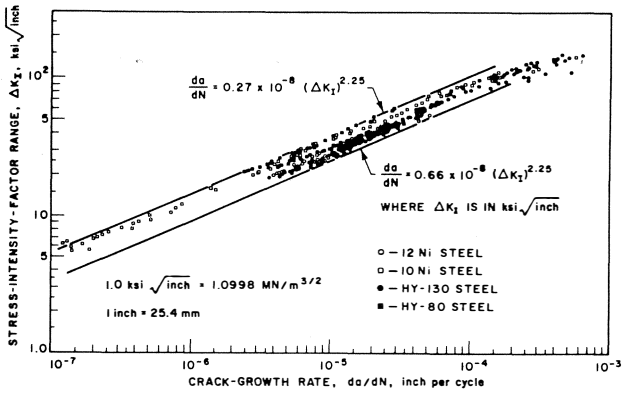

Figure 8. A Summary plot of Fatigue-Crack-Propagation for Martensitic Steels [16].

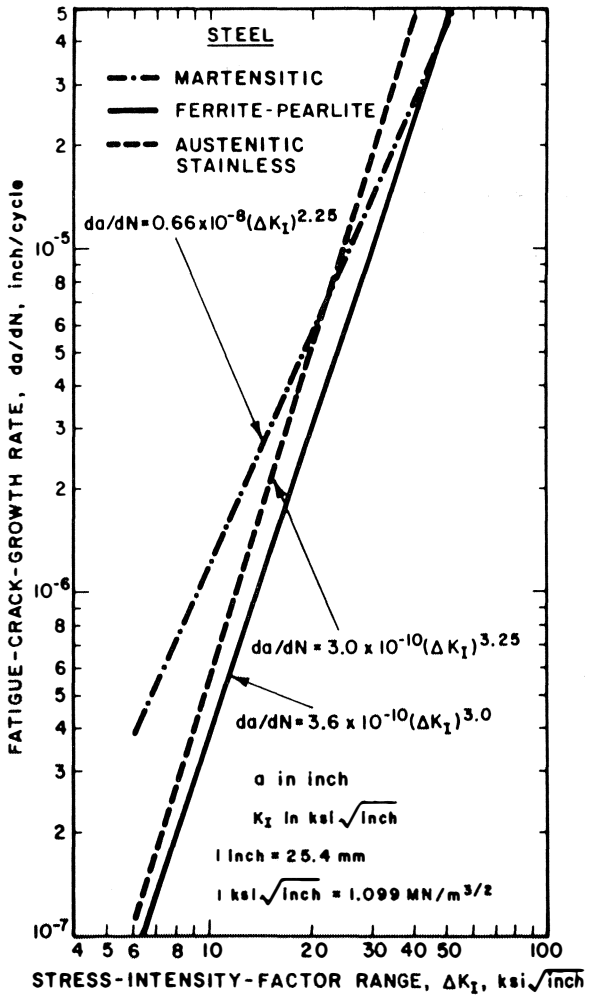

Figure 9. Comparison of Crack Growth Rates in Steels.

and exponent can be utilized for steels in general since this boundary is also conservative for ferritic and austenitic steels, as shown in Figure 9.

In order to get a better curve fit over a wider range of crack growth rates, Forman, et al. [17] put forth the following modified equation:

$$da/dN = \frac{C(\Delta K)^n}{(1-R)K_c - \Delta K} \quad (3)$$

where

R = cyclic ratio ($\sigma_{min} / \sigma_{max}$ or K_{min} / K_{max})
K_c = critical stress intensity factor for fracture, ksi $in^{1/2}$

This equation is still relatively useable without extremely involved calculations. However, it does not yield the sigmoidal curve shape over the widest range of crack growth rates and it does not introduce the threshold ΔK_0 level. The da/dN curve [18] for a Cr-Mo-V rotor steel is shown in Figure 10 to give an example of the true sigmoidal shape.

The Collipriest-Ehret [19] equation for the relationship between da/dN and ΔK does offer a sigmoidal curve, which contains the ΔK_0 level. It is as follows:

$$da/dN = C(K_c\,\Delta K_o)^{n/2} \exp\left[\left(\; n(K_c/\Delta K_o)\right)^{n/2} \text{arc tanh}\left[\frac{n\,(\Delta K^2/(1-R)\,K_c/\Delta K_o)}{n\,((1-R)\,K_c/\Delta K_\bullet)}\right]\right] \quad (4)$$

where

$\Delta K_\bullet$ = threshold cyclic stress-intensity level, ksi $in^{1/2}$

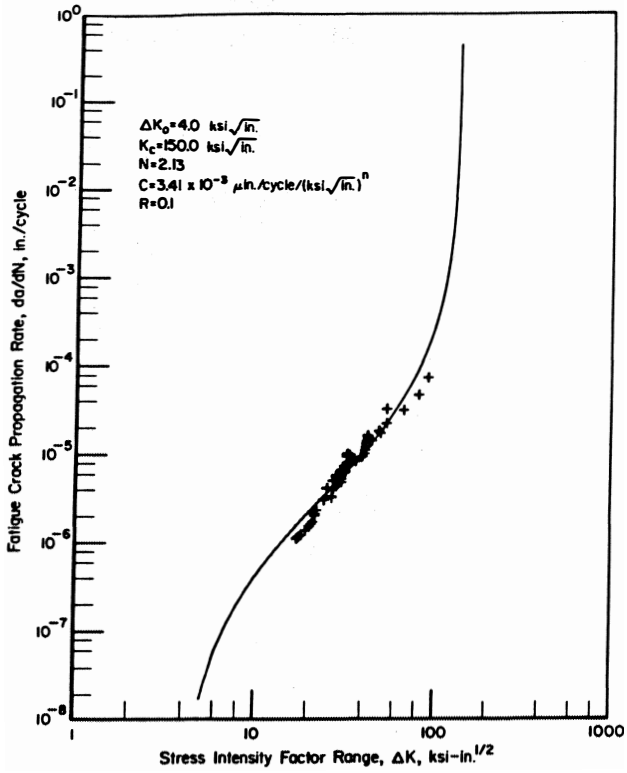

Figure 10. Fatigue Crack Growth Rate Behavior of Cr-Mo-V Steels at 250°F Yield Strength = 88.0 KSI [18].

One can readily see that a computer program is necessary to utilize Equation (4). There have been other equations developed and computer programs written to compute crack growth rate since this equation was proposed. The NASA/FLAGRO [20] program is probably one of the better known programs in aerospace applications. It can be configured to varying degrees of computation from the basic Equation (2) to equations which are far too involved for this presentation. There will be a new revision of NASA/FLAGRO available in the near future. This will differentiate the computation of crack growth rates for cyclic ratios greater than or equal to zero from those for cyclic ratios less than zero. Cyclic ratio, R, as defined in Equation (3) is known to give lower fatigue limits as the R value decreases from +1 to –1. This is shown graphically in the fatigue chart [21] for ASTM A517 steel in Figure 11.

Once the crack growth rate curve is known, it is possible to then predict the amount of crack extension that will be encountered for a flaw size geometry after so many cycles of loading. The solution will be based on a service spectrum and an assumption must be made of the various residual stress levels affecting the final flaw size after a given number of years. There is evidence [22] that the

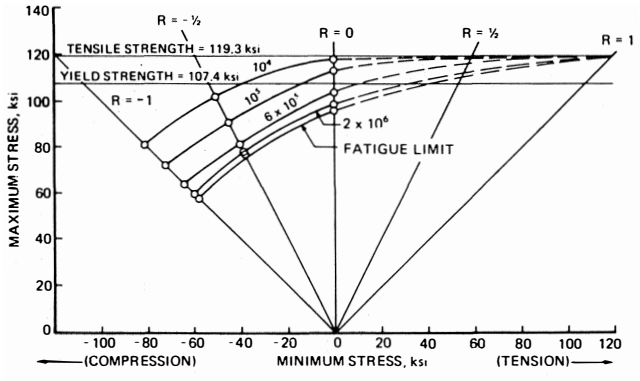

Figure 11. Fatigue Chart for Axially-Loaded, Polished Specimens of an ASTM A517 Steel [21].

fatigue crack growth rates in weld metal and in HAZ are equal to or less than that measured in the base metal. There are some other concerns that average levels of microscopic nonmetallic inclusions in the weld metal may prevent the weld metal from achieving higher fatigue strength as compared to that seen in the vacuum treated rotor steels [23].

A program was devised to investigate the weld metal properties for submerged arc weld metal in order to verify the concerns expressed by Clark, et al. [23]. The experiment and results obtained together with a discussion and conclusions are addressed herein.

EXPERIMENTAL METHOD

Submerged Arc Welding

Several experimental test assemblies have been made using submerged arc welding for rotor shaft restoration. The filler metals have been solid low alloy steel wire electrode with agglomerated granular flux of the lime-fluorspar composition. The submerged arc welding process can be readily mechanized to provide for smooth consistent travel speeds and even weld pass thickness and width. The wire electrode is usually connected to the positive side of the direct current power supply. The work is connected to the negative side. The welding arc is completely submerged in the granular flux. The flux, that is in close proximity to the welding arc, melts to entirely cover the molten weld metal pool and create a liquid-liquid interface. This is a very significant difference from other common welding processes which use gas to shield the molten weld pool and thus have a gas-liquid interface.

Because there is a liquid-liquid interface between the heavier molten weld metal and the lighter molten flux, it is possible to obtain very low wetting angles upon solidification. This directly affects the appearance of the final weld bead and yields a smooth, well tied in final weld surface. At the same time, the molten flux does provide a shield for the weld metal and prevents excessive entry of ambient air- oxygen and nitrogen. The molten flux also can remove some other contaminants from the weld metal.

However, it is always preferred to weld on a clean surface without excessive rust or greases and oils. The flux is a low hydrogen-generating flux when it is kept dry before use and is predried in a flux oven. If it is used to weld over grease or oil, these hydrocarbons will certainly breakdown with heat and render the welding system no longer low hydrogen. This flux also does not have high deoxidization capabilities since it is a basic flux. Fluxes that contain ferro-manganese-silicates have a higher tolerance for welding over rust. However, these fluxes are more acidic fluxes and do not give the lower inclusion count in the weld metal nor the better overall mechanical properties of the weld metal as compared to the basic flux systems.

Submerged arc welding as a process is position limited. Generally, the best weld appearance is obtained when the molten weld pool solidifies in the flat position. If the molten pool is slightly out of the flat position, the resulting weld will not attain the optimum bead appearance. This is shown in Figure 12. The loose granular flux that covers the welding arc must also be retained around the welding arc to shield the molten weld pool from the ambient air. When welding on a smaller diameter, two factors, solidification position and flux retention, are vital factors to producing a sound deposit with good bead wetting and tie-in. The base metal is rotated below the welding wire guide-contact tip. Flux is deposited either ahead of or around the wire electrode. The welding arc at the end of the wire electrode is usually positioned several degrees ahead of top dead center when welding in the circumferential direction around a smaller diameter cylinder. This allows the trailing edge of the molten weld pool to reach top dead center and solidify in the flat position. The welding arc force pushes the molten pool ever so slightly so as to keep it from flowing out of the leading edge of the weld pool. In order to retain the flux ahead of the welding arc, a flux dam is used to support the flux, as it is funnelled onto the weldment and, seconds later, melted by the welding arc.

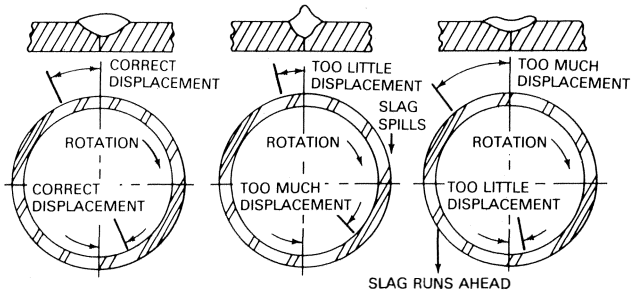

Figure 12. Sketch Showing Positioning of the Welding Arc for Circumferential Welding [24].

With larger diameters, the two factors of position and flux retention become easier to control because the exterior surface of the cylinder does not have the extreme curvature. The welding arc must still be offset or advanced a few degrees ahead of top dead center. In order to create a built up layer of weld metal, each pass is deposited in the circumferential direction on the girth of the cylinder with a slight overlapping translation every 360 degrees of rotation to produce a level layer of weld metal. The first layer adjacent to the base metal will have some base metal diluted into the filler metal deposited. This mixture results in a homogeneous composition of weld metal in the first layer. The second layer added on top of the first layer will have some of the first layer diluted into the filler metal to form the second layer. By the time the third layer is welded, the composition will be that of the filler metal with very little dilution effect from the base metal.

Journal Mock Up Repair Test

The original Elliott test assembly for submerged arc restoration of a rotor shaft was reported in 1986 [25]. Prior to this, most rotor shaft repairs were made using either manual gas tungsten arc welding or manual shielded metal arc welding, usually to correct machine tool gouges. Preheating and postweld heat treating were done on the heat indicating lathe. The first test assembly for submerged arc restoration was a mock up test on a bar of AISI 4340 low alloy steel in the quenched and tempered condition. It was done to qualify the new procedure for journal repairs on axial compressor rotor shafts which had experienced bearing failure resulting in heavily scored shaft journal areas. The experimentation was monitored by an insurance inspectorate and samples of the weld test were sent to the engineering consultant for verification of results and fatigue testing.

The test was performed on a 6.0 in diameter bar of AISI 4340, 28 in (700 mm) long, which was cleaned and inspected prior to welding. This simulated shaft was set in a rotational positioner-lathe and heated to 500°F (260°C) while being rotated. Once the preheat temperature was fully soaked through the bar, a submerged arc weld buildup was applied along 18 in (450 mm) of the length to a final weld diameter of 9.0 in to permit test sample removal. The remaining 10 in (250 mm) length was weld built up with three layers to be used to make the actual journal restoration. The filler metal used to weld this test assembly was one that is used to weld HY-80 steel (Mil-S-16216). It is lower in carbon and chromium content than AISI 4340, which improves its weldability. The filler metal is higher in manganese, molybdenum and vanadium, which gives it comparable strength and secondary hardening characteristics. This filler metal had previously been used in a submerged arc welding development project for fabrication of welded axial rotors in 1983.

Postweld heat treatment was performed after the assembly had slowly cooled to room temperature. The sample was machined to the required diameters of 10 in (250 mm) and the final journal diameter. A hardness survey was taken across the weld prior to heat treatment. Fluorescent magnetic particle examination was also performed. The postweld heat treatment was performed at 1100°F (593°C) for 10 h in a pit furnace. After postweld heat treatment, specimens were removed by mechanical cutting in order to test for hardness, all-weld-metal tensile strength, base metal tensile strength, weld metal chemistry, longitudinal base metal impact strength, weld metal, and HAZ impact strength in both longitudinal and radial orientations. Guided bend specimens were also taken in four quadrants in the weld-fusion line- HAZ area to check for bending ductility.

First Disc Mock Up Weld Test

The first disc mock up weld test assembly was fabricated using an ASTM A470 Class 8 forging that was 10 in (250 mm) in diameter and 24 in (600 mm) long. This test piece was undercut to an 8.0 in (200 mm) diameter, 5.0 in. (125 mm) wide to allow a foundation weld buildup to be made first. Once the foundation buildup was complete and inspected for cracks, a disc buildup was placed on the foundation up to a final finished diameter of 22 in (550 mm), as shown in Figure 13. This was done in two to four iterations by welding successive layers up to a point where the weld metal cannot be piled any higher. At this point, the weld is cooled to room temperature slowly allowing time for the weld to outgas. The buildup is rough machined and inspected. Then the top is adapted to take the next sequence of layers. The total number of passes required to lay the foundation buildup and complete the disc buildup to the 22 in (550 mm) diameter was 1495 weld passes. The total number of layers was 95 with each layer averaging 0.074 in (1.95 mm) thick. The number of passes per layer varied from between 18 and 25 passes per layer in the foundation buildup to between 14 and 17 passes per layer in the disc buildup. This mock up test assembly was final inspected with both penetrant and ultrasonic testing. The final postweld heat treatment was performed in a subcontract facility. Unfortunately, it was later discovered that the subcontract heat treat facility overran the required soaking temperature by five to ten percent, which rendered the test piece worthless as far as mechanical testing. The test piece was sectioned and polished to show an overtempered and partially austenitized microstructure. This lost test piece only confirmed the high degree of control necessary when postweld heat treatment is being done near the transformation temperature of the weld metal.

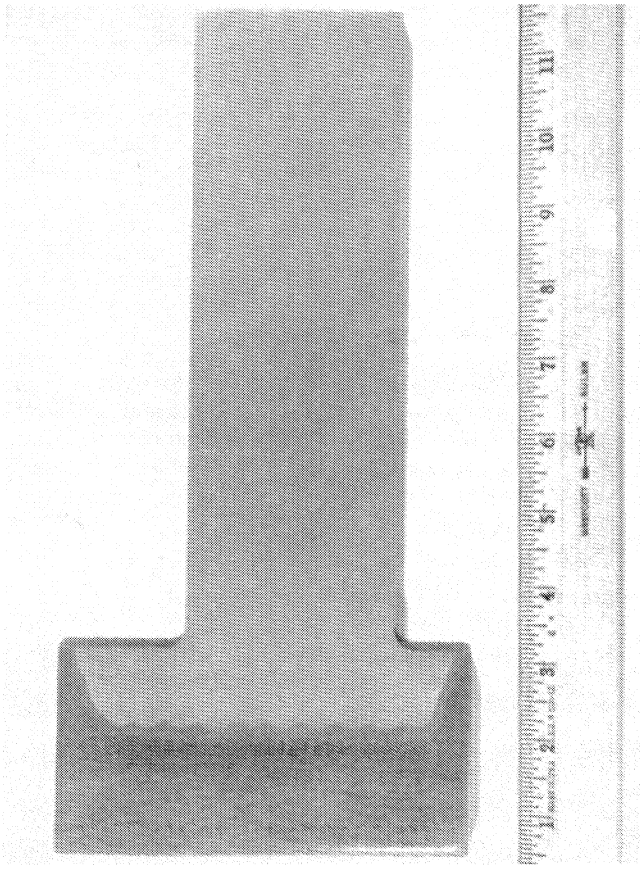

Figure 13. The Polished and Etched Crosssection of the Thick Disc Buildup.

Second Disc Mock Up Weld Test

In order to salvage this mock up test phase, another foundation and disc buildup was made on a 23 in (575 mm) long piece of hot rolled AISI 4140 shaft material in the quenched and tempered condition. This buildup was made in the same manner with the high strength submerged arc filler metal usually used to weld ASTM A514/ A517 high strength quenched and tempered steels. However, the shaft diameter was 8.25 in (210 mm) and once undercut for the foundation buildup, the initial layer was deposited on the 6.0 in (150 mm) diameter. Once the 5.0 in (125 mm) wide foundation buildup was complete the disc buildup was commenced. The disc buildup was deposited 2-1/2 in (64 mm) wide by 22 in (550 mm) in diameter. The total number of layers was 119 with 2004 passes to achieve the total buildup. The preheat and interpass temperature was held between 600°F (315°C) and 750°F(399°C). When this buildup was completed, it was fully inspected with magnetic particle and ultrasonic testing. The mock up test assembly was postweld heat treated locally using resistance heater blankets and computer-controlled power supplies equipped with monitoring thermocouples. The test assembly was also given a second postweld heat treatment under close supervision in the laboratory. This mock up test assembly provided all the weld metal test specimens for the fatigue testing, elevated temperature tensile testing, chemical analysis, hardness testing, impact testing and radial direction stress rupture testing.

Weld Buildup Test

At the same time, weld test assemblies were made with 3.0 in (75 mm) by 6.0 in (150 mm) forged bars of ASTM A470 Class 8. Each bar was 18 in (450 mm) in length. A weld buildup was deposited on one of the 3.0 in (75 mm) wide sides of each bar with the weld length running parallel with the 18 in (450 mm) length. The buildup was made to a height of 1.5 in (38 mm) to permit removal of heat affected zone Charpy specimens. The preheat and interpass temperature was held to the same limits as the previous test. The final postweld heat treatment was performed in the laboratory with the soaking temperature the same as the second heat treatment given the second mock up weld test assembly. Both the second mock up weld test assembly and the weld buildup test assembly were nondestructively tested with penetrant testing, magnetic particle testing, and ultrasonic testing, using longitudinal and shear wave technique. No defects were found.

RESULTS OF TESTING AND EVALUATIONS

Journal Mock Up Repair Test

Electrical and Mechanical Runout

Testing of the mock up test for journal repair on a bar of AISI 4340 was done in conjunction with an engineering consultant. Elliott Company performed all the mechanical, chemical, runout, and hardness testing. The engineering consultant performed the fatigue testing. Dowson [25] reported that the smaller diameter, three pass weld buildup to simulate the actual repair of a shaft journal, could be held within 0.5 mil (0.013 mm) electrical and mechanical runout, if burnishing was used in the finishing of the journal area. However, the area of the shaft that was built up to the 10 in (250 mm) diameter with a 2.0 in (50 mm) thick buildup of weld metal would not respond to burnishing and a 1.5 mil (0.039 mm) electrical runout value was the best that could be achieved. Therefore, heavier thickness buildup in areas that require close control of electrical runout was not recommended.

Chemistry and Mechanical Properties

The chemical analysis of the weld metal deposit for journal repair showed an extremely low carbon level for a high strength low alloy weld deposit. This is beneficial for thin deposits where the pickup of carbon from dilution of the weld metal with the much higher carbon base metal was a major concern. However, once above the third layer there was a concern that this weld metal would not exhibit good high strength properties. Subsequent hardness testing and mechanical testing did confirm this. The hardness data showed the final weld layers in the heavy deposit region were 97 Rockwell "B." The region of the third layer was approximately 22 Rockwell "C." The mechanical testing of the weld metal in comparison to the base metal are shown in Table 1. The all weld metal values were less than the base metal values for tensile and yield strength. However, the ductility and toughness of the weld metal was far greater than the base metal. Guided bend testing of the fusion line region which included heat affected zone (HAZ) showed clean sound metal as shown in Figure 14.

Fatigue Testing

The cyclic rotating beam fatigue data from the engineering consultant showed thirty samples being tested (fifteen weld and fifteen base metal). These were tested at room temperature in air at 60 Hz with complete reversal of stress. The data are plotted and shown in Figure 15 for base metal and in Figure 16 for the weld metal. Fuentes and Hodas [26] reported that the endurance limit for the base metal is approximately 60000 psi (414 MPa) and for the weld is approximately 55000 psi (379 MPa). The final decision based on all this data was that the HY80 type filler metal would be adequate for journal repairs. However, another filler metal should be found for the heavier buildup. Therefore, when the mock up weld test assembly was made a filler metal was selected with a minimum limit of carbon.

Table 1. Mechanical Properties of Weld Metal Used in Journal Mock Up Repair Test.

	Yield Strength, 0.2% Offset (ksi)	(MPa)	Tensile Strength (ksi)	(MPa)	Elongation in 2 in. (%)	Reduction of Area (%)
Base Metal	110	758	133	917	20.5	57.6
All-Weld-Metal	83	572	102	703	27.5	67.9
All-Weld Metal 2	84	579	102	703	27.5	70.8
AISI 4340 (min. value)	90	621	115	793	16.0	45.0

Charpy V-Notch Impact Values at 68°F(20°C) Test Temperature

		Energy (ft-lbf)	(J)	Lateral Expansion (mil)	(mm)
Transverse base metal	1	26.5	36	19.9	0.51
	2	26.0	35	17.5	0.44
	3	26.5	36	20.0	0.51
Longitudinal Base Metal	1	57.5	78	41.5	1.05
	2	58.5	79	38.5	0.98
	3	59.5	80	39.0	0.99
Transverse HAZ	1	34.0	46	24.0	0.61
	2	47.0	63	34.0	0.86
	3	44.0	59	29.5	0.75
Longitudinal HAZ	1	57.0	77	34.5	0.88
	2	60.0	81	35.0	0.89
	3	56.5	76	33.5	0.85
Transverse weld metal	1	130.5	176	79.0	2.01
	2	140.0	189	84.5	2.15
	3	120.5	163	70.0	1.78
Longitudinal weld metal	1	129.0	174	76.0	1.93
	2	139.0	188	74.0	1.88
	3	127.0	171	69.5	1.77

(All test specimens were prepared and tested per ASTM A370 Standard)

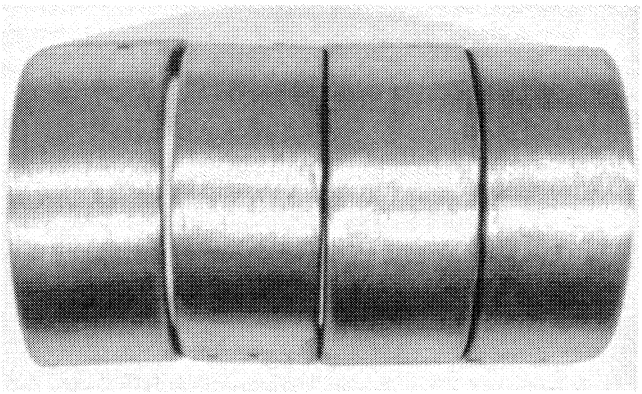

Figure 14. Guided Bend Test Specimens from the Journal Mock Up Repair Test Assembly.

Disc Mock Up Weld Test

Weld Deposit Consistency

The chemical analysis of the disc mock up weld test assembly deposit, that measured 9.0 in (225 mm) in overall weld deposit thickness, showed very little variation in chemical composition from the center of the foundation buildup to the top of the disc buildup. The amount of variation for each element is shown in Table 2 along with the percentage increase or decrease from the normal amounts. Only four chemical elements showed any signif-

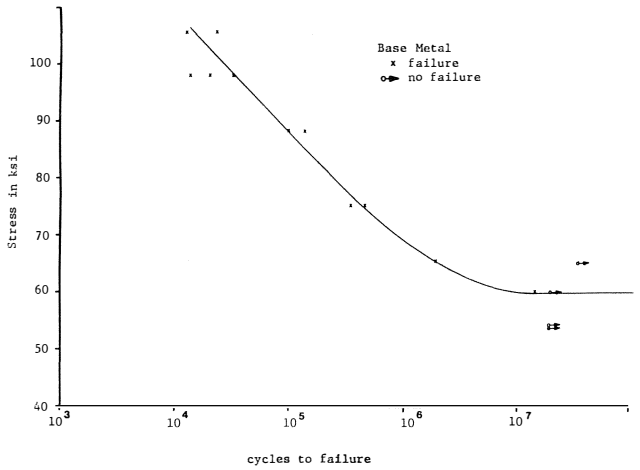

Figure 15. S-N Curve for Base Metal from Journal Mock Up Test [26].

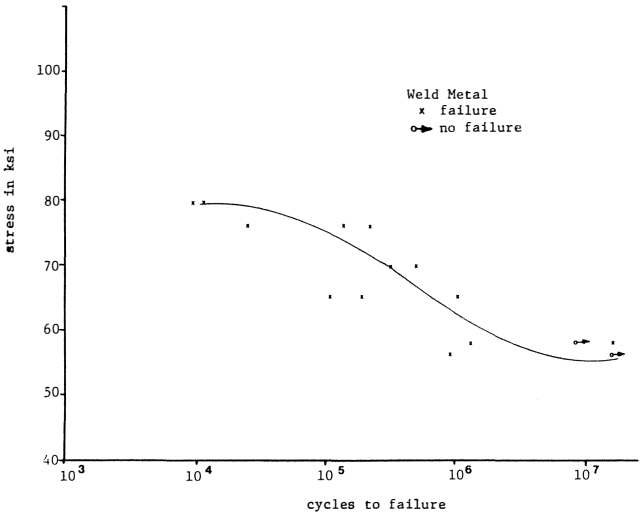

Figure 16. S-N Curve for Weld Metal from Journal Mock Up Test [26].

icant variation from bottom to top of the deposit. Carbon, manganese, and chromium decreased from six to fifteen percent of the base amount in the deposit. However, the carbon level in this extremely heavy deposit was still almost double that attained in the previous journal repair test assembly. Silicon amount increased by 20 percent of the base amount in the weld metal deposit. All other elements measured showed very little change from the bottom to the top of the weld deposit.

The measured hardness of the weld metal deposit was very consistent, as shown in Figure 17. The hardness was measured in

Table 2. Variance in Weld Metal Chemical Composition from Bottom to Top of the Heavy Disc Buildup Weld.

	Carbon	Manganese	Silicon	Chromium	Other Elements
Variance, % by wt.	−0.015	−0.09	+0.05	−0.02	0.01
Percentage, + or −	−15%	−6%	+20%	−6%	N.A.

Rockwell "B" and only varied from readings of 98 to 100. This is considered to corroborate the very small variance in the chemical composition shown in the weld metal deposit.

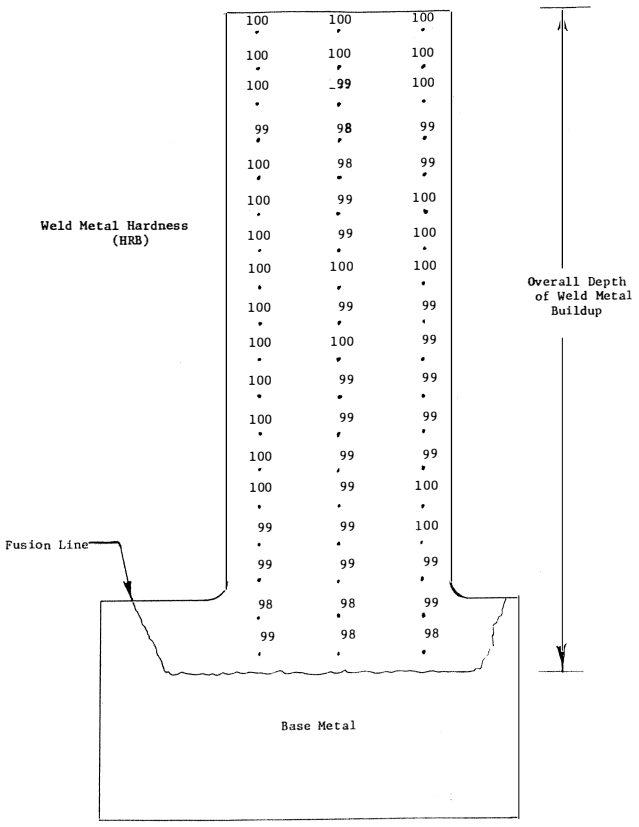

Figure 17. Layout of Hardness Readings in the Disc Mock Up Test.

All-Weld-Metal Tensile Testing

Tensile testing results are shown in Figure 18. These include room temperature and elevated temperature tensile test results. The yield strength is plotted with the values obtained with 0.2 percent offset. Values of yield strength measured with 0.02 percent offset were generally 10000 psi (69 MPa) less than the values plotted in Figure 18. The elongation percentage plotted is determined using a 2.0 in (50.8 mm) gauge length. All data was obtained by using a standard 0.505 in (12.83 mm) diameter turned specimen in accordance with ASTM A370 Standard. These turned tensile specimens were all taken entirely from the mock up weld deposit with the specimen axis oriented in the radial direction on the disc buildup.

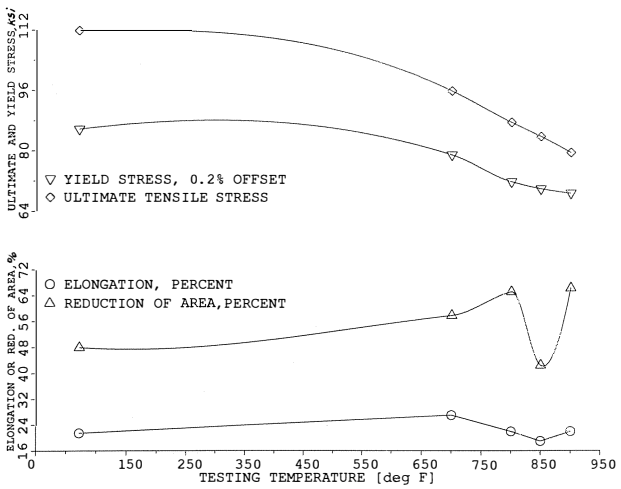

Figure 18. Elevated and Room Temperature Tensile Test Results.

In order to evaluate the mock up weld deposit for directional variation in mechanical strength properties, additional room temperature tensile tests were made, utilizing 0.252 in (6.42 mm) diameter turned tensile specimens. The axially-aligned tensile specimens taken at the outer diameter or top of the weld deposit gave slightly higher values of ultimate tensile strength and yield strength than the axially-aligned tensile specimens taken down near the transition radius at the foundation buildup. The same trend existed with the tangentially-aligned tensile specimens taken near the outer diameter of the mock up weld deposit and the ones taken down near the transition radius. These data are shown in Table 3. The difference from top to bottom is only four percent of the strength level measured. The difference from axially-aligned to tangentially-aligned specimens on a given diameter of the weld deposit is insignificant.

Table 3. Comparison of the Tensile Test Results of Axially-Aligned and Tangentially-Aligned All-Weld-Metal Specimens from the Top and Bottom of the Heavy Disc Mock Up Weld Deposit.

Specimen No.	Alignment	Location	Yield Strength ksi	(MPa)	Tensile Strength ksi	(MPa)
AW-1	Axial	Top	87	(600)	114	(786)
AW-2	Axial	Top	86	(593)	114	(786)
AW-3	Axial	Bottom	83	(572)	111	(765)
AW-4	Axial	Bottom	83	(572)	110	(758)
TW-1	Tangential	Top	87	(600)	115	(793)
TW-2	Tangential	Top	87	(600)	115	(793)
TW-3	Tangential	Bottom	83	(572)	113	(779)
TW-4	Tangential	Bottom	85	(586)	113	(779)

All-Weld-Metal Charpy V Notch Impact Testing

Nine Charpy impact specimens were first tested at 250°F (121°C), in order to evaluate the toughness of the mock up weld deposit at the top (outer diameter), middle and bottom (transition radius). These Charpy impact specimens had their major dimension aligned in the radial direction, so that the fracture occurred in a plane parallel with the welding layers. All the specimens impact tested at 250°F (121°C) exhibited 100 percent shear with upper shelf energy levels in excess of 120 ft-lbf (162 J). There was a slight variation in the energy levels attained with the specimens taken at the top (outer diameter) as compared to the energy levels attained with specimens at the middle or at the bottom of the disc buildup (transition radius). The Charpy impact energy values from the specimens taken near the transition radius gave on the average 10 ft-lbf (13 J) higher results than the specimens taken out nearer the outer diameter.

Three axially-aligned Charpy specimens taken from the top (outer diameter) of the mock up weld deposit were also tested at 250°F (121°C). Again, these specimens all exhibited 100 percent shear, but the impact energy levels were about 10 ft-lbf (13J) less than the energy levels obtained with the radially-aligned Charpy specimens taken from the outer rim weld metal.

Fracture Appearance Evaluation of Weld Metal

In order to test the weld metal to determine the $FATT_{50}$ of the weld deposit in the disc buildup, it was necessary to make six sets

of Charpy V-notched specimens from the disc buildup material. These were all removed in such a manner as to have the major axis aligned in the radial direction. Each set consisted of three specimens with one specimen from each level in the disc buildup. This arrangement was selected to minimize the effect of specimen location that was discussed earlier with the radially-aligned specimens impact tested at 250°F (121°C). Each set of specimens was impact tested at different temperature levels to finally arrive at a temperature that approximates the $FATT_{50}$. The resulting data are shown on Figure 19, along with the original radially-aligned specimen data taken at 250°F (121°C). The $FATT_{50}$ of the weld metal is approximately –15°F (–26°C). The upper shelf Charpy V-notch energy levels for this weld metal are approximately 120 to 140 ft-lbf (162 to 189 J). The energy levels at the $FATT_{50}$ are approximately 55 to 65 ft-lbf (74 to 88 J).

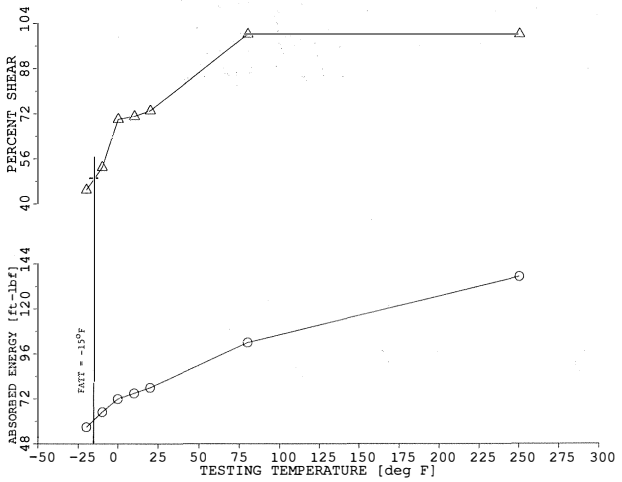

Figure 19. Charpy Impact Energy as a Function of Test Temperature for Weld Metal Used in Disc Mock Up Test.

All-Weld-Metal Stress Rupture Testing

The stress rupture testing of the weld metal was performed using notched turned specimens in accordance with ASTM A370 Standard. These specimens were tested at three temperatures—800°F (427°C), 850°F (454°C), and 900°F (482°C). A few of the ruptured test specimens are shown in Figure 20. The stress rupture data gathered yielded the curve shown in Figure 21. A standard base metal curve for ASTM A470 Class 8 forged material is shown in Figure 22. The weld metal and the base metal rupture strength at 10000 hr is plotted for various temperatures and is shown in Figure 23. Weld metal stress rupture data for 100,000 hr were not available at the time of this report. It is expected to be available in 1996.

Weld Buildup Test

Heat Affected Zone Hardness

The microhardness in the weld metal-HAZ-base metal region on the weld buildup test assembly using ASTM A470 Class 8 base metal is shown in Figure 24. The peak hardness occurs in the HAZ, as expected. An additional postweld heat treat cycle was made on this test assembly and the hardness peaks did decrease by about three points on the Rockwell "C" scale.

Heat Affected Zone Charpy Impact Testing

Three Charpy V-notched specimens were taken from the heat affected zone region of the weld buildup test assembly using the

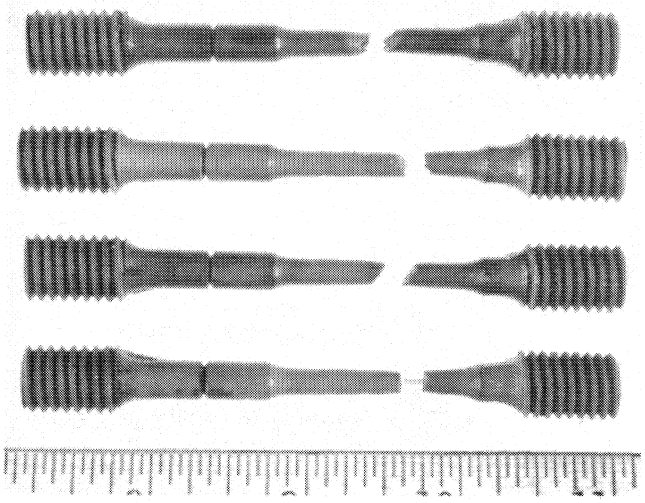

Figure 20. A Selection of Ruptured Test Specimens Used to Determine Stress Rapture Strength in the Weld Metal of the Disc Buildup.

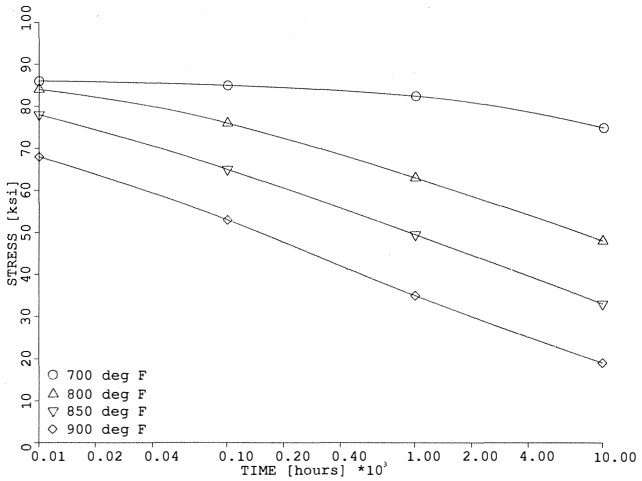

Figure 21. Weld Metal Stress Rupture Curves at Various Temperatures.

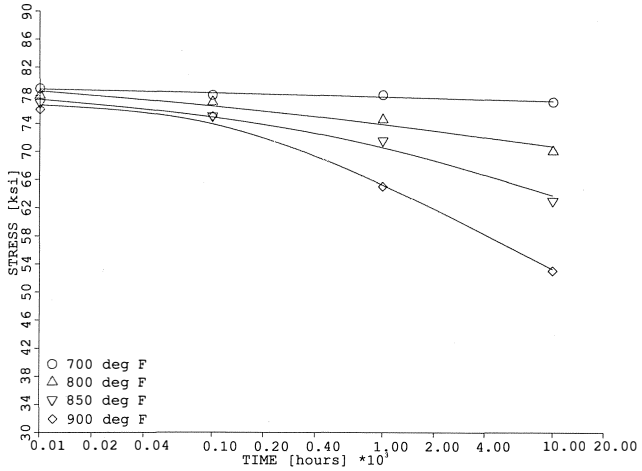

Figure 22. Standard Stress Rupture Curves for ASTM A470 Class 8.

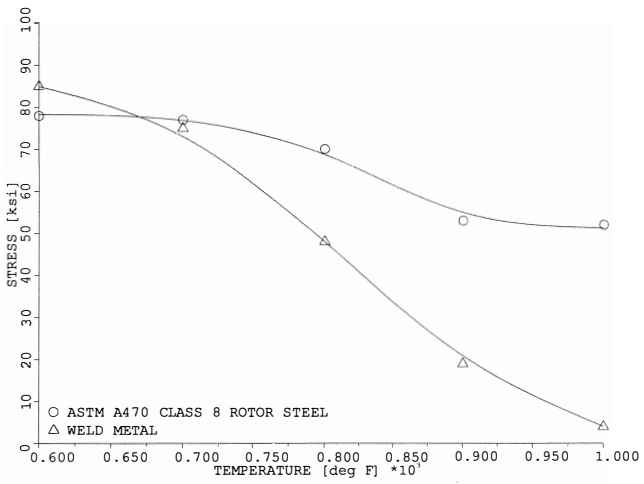

Figure 23. Stress Rupture Strength of the Weld Metal and the Base Metal as a Function of Temperature at 10000 Hr Loading.

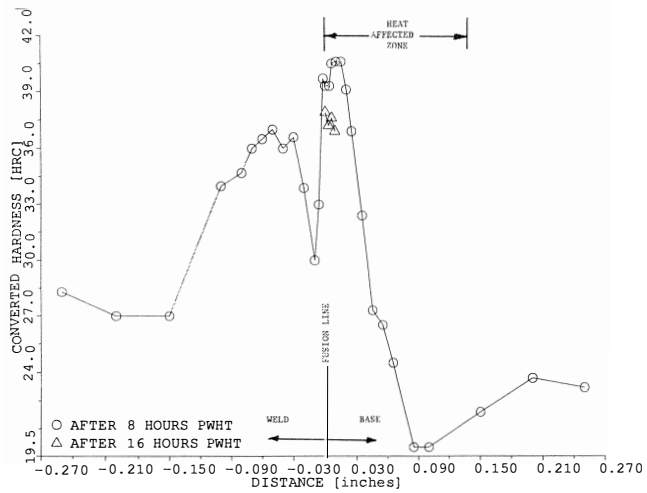

Figure 24. A Plot of the Converted Microhardness Readings at Various Locations on the Weld/Heat Affected Zone/Base Metal Region after Postweld Heat Treatment.

ASTM A470 Class 8 forged bar base metal. These test specimens also exhibited 100 percent shear when impact tested at 250°F (121°C), and showed energy levels of the same magnitude as the levels seen in the impact tests on the weld metal from the mock up weld test assembly.

Fatigue Testing of Weld Metal and Base Metal

The fatigue testing of the weld metal and the base metal was done using the rotating beam specimen with complete reversal of stress. The testing was done in air at room temperature at 167 Hz. Twenty-five weld metal tests and 12 base metal tests were run at stress levels varying from 75 ksi (517 MPa) bending stress down to 50 ksi (345 MPa) bending stress. The maximum number of cycles achieved was 100 million. The base metal showed an endurance limit of approximately 60000 psi (414 MPa) at 10 million cycles. The weld metal endurance limit was approximately 50000 psi (345 MPa) at 100 million cycles. These data are shown in the S-N curve in Figure 25. Some of the weld metal fatigue specimens tested did fracture at lower stress levels with only 300 000 cycles. A scanning electron micrograph of one these fractures is shown in Figure 26. Small nonmetallic inclusions measuring 8 mil (0.20 mm) in diameter, that happened to be near the finished surface of the specimen, appear to have shortened the crack initiation stage of fatigue testing. This resulted in a much shorter number of cycles to failure than was measured with other weld metal fatigue specimens, where the nonmetallic inclusions were not near the finished surface.

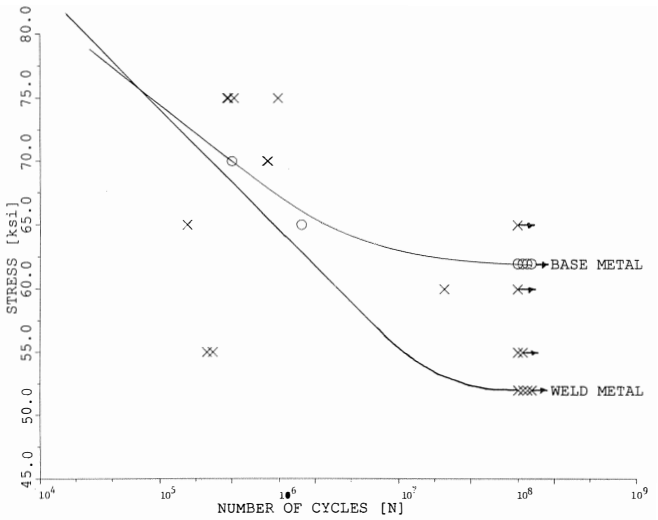

Figure 25. S-N Curve for the Weld Metal from the Disc Mock Up Weld Deposit.

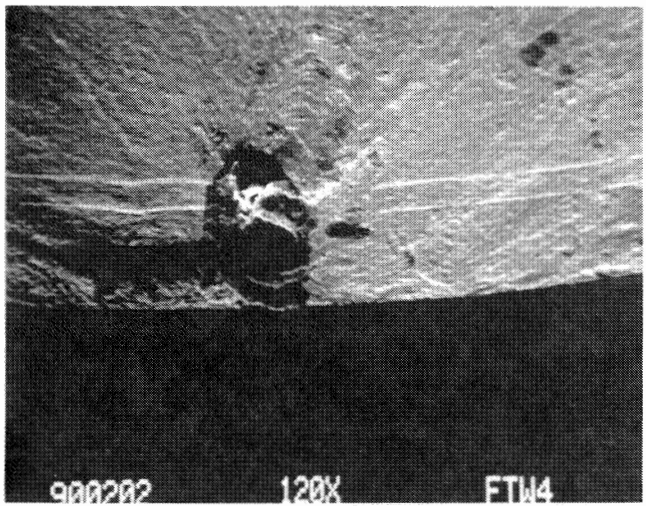

Figure 26. Scanning Electron Micrograph of Nonmetallic Inclusion in Fractured Surface of Fatigue Specimen.

DISCUSSION OF RESULTS

Journal Mock Up Repair Test

The results from the journal repair weld buildup on AISI 4340 showed that a very sound deposit of high strength weld could be accomplished on a small diameter journal area in order to restore the bearing surface. The strength levels in the weld metal were adequate for journal and seal areas. The ductility and the toughness was equal to that normally obtained in the base metal. The electrical and mechanical runout, although thought to be a marginal problem, has not proven to be a problem in the dozens of welded journal repairs made since these original tests were performed. Welded journal repairs have become almost a routine repair

procedure for compressor rotors of AISI 4130, 4140, and 4340 base material. In addition, journal repairs have been performed on several steam turbine rotors of ASTM A293 or A470 materials with excellent final results. These have all gone back into service with electrical and mechanical runout within the 0.5 mil requirement.

Disc Mock Up Weld Tests

Variations Within the Thick Weld Deposit

The disc mock up test assemblies clearly demonstrated the possibilities achievable with heavy thickness, submerged-arc-welded deposits. Although the first test assembly was rendered useless due to heat mistreatment by an outside commercial heat treater, the second mock up test assembly proved to be very consistent from top to bottom with regard to chemistry of the weld deposit, hardness, and overall quality of the fusion within the deposit. There was only a slight variation in the strength of the weld metal from the top (outer diameter) to the bottom (transition radius). The weld metal at the top of the deposit was four percent higher in strength than the weld metal at the bottom. The toughness of the weld metal as measured with Charpy V notch specimens was slightly tougher at the bottom of the deposit than at the top. The directions, in which the specimens were taken, did not give significantly varying results.

Weld Metal Yield Strength

The weld metal yield strength at 0.2 percent offset gave values from 82 ksi (565 MPa) to 87 ksi (600 MPa). This is 10 to 15 percent less than the room temperature minimum yield strength of the ASTM A470 Class 8. This same trend was evidenced at 0.02 percent offset. The weld metal yield strength declined to 78 ksi (538 MPa) when tested at 700°F (371°C). Upon testing at 900°F (482°C), the weld metal yield strength was down to 68 ksi (469 MPa). These results indicated that the weld metal stress rupture testing should be in this temperature range.

The lower yield strength in the weld metal is not totally surprising when considering that the base metal contains two to three times more carbide forming alloying elements together with three times more carbon then the weld metal. This additional alloying will influence the retention of strength after the tempering heat treatment. A weld metal with higher carbon could be used. A weld metal with higher carbon, chromium, molybdenum, and vanadium could also be used. However, one may suddenly find that these additional alloying quantities will affect the weldability to the point of getting marginal results from the standpoint of weld metal cracking. It is better in these circumstances to maximize ductility and toughness and nominally attain the minimum strength required for the engineering design. This is a design concept is well understood but does require competent engineering judgement.

Comparative Fracture Toughness

The upper shelf impact strength of the weld metal was 30 percent higher than the base metal at 250°F (120°C). At room temperature, there was an even more marked difference with the weld metal impact strength at 90 ft-lbf (122 J) and the base metal registering 15 ft-lbf (20 J). This difference would account for almost a 100°F (55°C) shift in the dynamic critical stress intensity curve comparing the weld metal with the base metal. This is certainly maximizing the toughness of the weld metal as compared to the base metal. If the correlation, given earlier as Equation (1), were used to estimate the critical plain-strain stress-intensity factor, K_{Ic}, of the weld metal, the estimated value would be 225 ksi in1/2 (247 MN $m^{-3/2}$). This is extremely high for most steels and is characteristic of a metal which can take high crack tip strains without catastrophic rupture.

Comparative Stress Rupture Strength

The stress rupture testing of the weld metal is necessary to evaluate the opposite characteristic. Under static tensile loading at elevated temperatures, how long can the metal specimen sustain the load without rupture? In this case, the base metal is designed to outperform the weld metal by at least a couple of hundred degrees. The question utmost in consideration was what is the upper limit temperature for the weld metal? Empirically, this had been set at 650°F (343°C) prior to actually performing the stress rupture testing of actual weld metal. It turned out that this empirical limit was not far off from the experimental value of 680°F (360°C). Therefore, by continuing to apply the original empirical limit, the weld metal will be safe. To operate above 680°F (360°C), then serious consideration must be given to maintaining lower stress levels in the area to be repaired, so that the minimum creep strength is not exceeded.

Weld Buildup Test

Heat Affected Zone Hardness

The high hardness values found in the heat affected zone of the ASTM A470 Class 8 are indicative of the self-quenching effect of the base metal. The base metal in this case is hardenable and the 600°F (316°C) preheat temperature has certainly retarded this quenching effect. However, even long term tempering has not been sufficient to bring the maximum HAZ hardness below a converted microhardness of 35 HR C.

Heat Affected Zone Toughness

The gain in upper shelf Charpy impact values in the HAZ as compared to the values of the unaffected forged bar base metal reported by the vendor are of particular concern. This same result was found by Saha and Conway [4] in their report on Shawville #4 rotor repair. Considerably more needs to be done to investigate the HAZ of the rotor steels. This could be done independent of welding by the use of an instrumented weld heat affect simulator.

Fatigue Strength

The fatigue testing results of radial specimens from the disc buildup exhibited much the same general characteristics as found by Fuentes and Hodas [26] on the fatigue specimens from the journal repair buildup. The weld metal from the disc buildup had an endurance limit of approximately 52000 psi (361 MPa), and the base metal had an endurance limit of approximately 60000 psi (417 MPa). This fatigue testing was done with the full 100 million cycles, whereas the previous fatigue testing of the journal mock up repair test was only tested to 10 million cycles.

The influence of the microscopic nonmetallic inclusions on the crack initiation stage of the fatigue test was a bit surprising. Specimens that should have sustained 30 million cycles failed in 300,000 cycles. This hundred fold decrease in fatigue life under complete reversal stress would be cause for some concern in severe stress reversal applications, where the stress ratio, R, in Equation (3) is less than zero. In a well balanced rotor shaft, there is little likelihood of stress reversal and the R value is unlikely to be less than zero. Therefore, the rotating beam type of fatigue testing may be too severe a condition by which to judge the fatigue limit of the weld metal in this application.

These microscopic nonmetallic inclusions were scanned for comparative spectrographic analysis using a scanning electron microscope equipped with an X-ray analyzer using the energy dispersive technique. This scan is shown in Figure 27. The principal element found is calcium, which is the primary element in the lime-fluorspar submerged arc welding flux. A comparative scan was also made of some fused flux chipped from the top of a weld.

This is shown in Figure 28. It is clear that the microscopic nonmetallic inclusion is resultant from welding slag that was trapped in the solidifying weld metal. These microscopic slag inclusions, if brought near to the surface by machining, can become a surface flaw which may propagate under severe cyclic load.

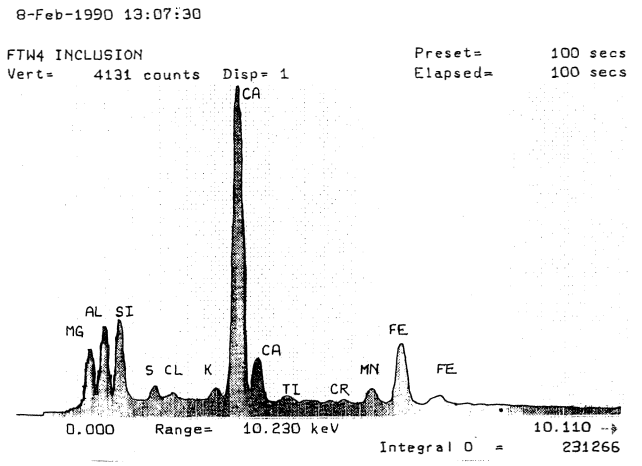

Figure 27. X-Ray Analyzer Scan of the Nonmetallic Inclusion Found in a Weld Metal Fatigue Specimen.

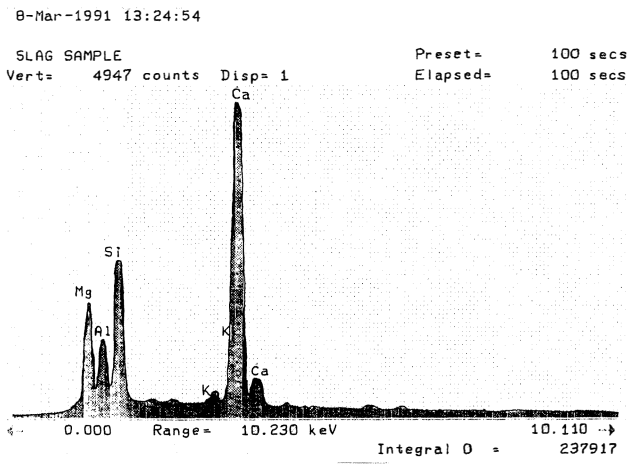

Figure 28. X-Ray Analyzer Scan of a Sample of Fused Slag Chipped from the Top of a Completed Submerged Arc Weld Pass.

CONCLUSION

Submerged arc welding offers an effective means of repairing damaged or cracked areas on monoblock turbine rotor shafts. It also can be used on compressor shafts of AISI 4100 and 4300 series steels in the quenched and tempered or normalized and tempered condition. Submerged arc welding can produce weld metal which has:

- Consistency in chemistry and hardness in deposit thicknesses up to 9.0 or 10 in (225 to 250 mm),
- Sufficient tensile and yield strength to meet the engineering design of many rotors,
- Sufficient fracture toughness to equal or exceed the toughness of the base metals used in rotor shafts, and
- Sufficient stress rupture strength to equal the base metal stress rupture strength up to a metal temperature of 650°F (343°C) for 10000 hr service.

Although the fatigue testing of the weld metal showed some weaknesses due to small inclusions in the weld metal, the rotating beam type of fatigue testing is a more severe condition than is usually seen in a well balanced rotor shaft. An axially-loaded, low cycle fatigue test with a precracked or notched specimen would give a more meaningful evaluation of the weld metal fatigue strength as it relates to the rotor shaft application.

A university is preparing double cantilever beam specimens of the weld metal, base metal, and heat affected zone, if possible, in order to obtain a K_{Iscc} value for each. The test medium will be caustic with a chloride content between one percent and four percent, heated to 212°F (100°C).

There is a need to perform more testing of the weld metal-HAZ-base metal transition zone in the various rotor steels. This can be done using weld buildup test assemblies similar to that used in this experimentation; or, a weld heat simulator could also be used to duplicate the heat affected zone in various base metals. More needs to be known as to the stress rupture strength, FATT, and fatigue strength of the heat affected base metal. The experience with submerged arc weld restoration of turbomachinery rotors to date indicates that the successes far outweigh the disadvantages and that future developments will yield even better results.

REFERENCES

1. Bertilsson, J. E., Faber, G., and Kuhnen, G., "50 Years of Welded Turbine Rotors," Brown Boveri Review, pp. 467- 473 (December 1981).
2. Swaminathan, V. P., Steiner, V. P. and Jaffee, R. I., "High Temperature Steam Turbine Forgings by Advanced Steel Making Technology," ASME Paper No. 82-JPGC-Power-24, Denver, Colorado (October 1982)
3. Kotecki, D. J. and LaFave, R. A., "AWS A5 Committee Studies of Weld Metal Diffusible Hydrogen," Welding Journal, 64 (3) pp. 31-37 (March 1985).
4. Saha, S. K. and Conway, J. F., "Weld Repair of Shawville #4 LP Rotor," Proceedings of Seminar on Life Assessment and Improvement of Turbo-Generator Rotors for Fossil Plants, Raleigh, North Carolina, EPRI CS-4160, Ed: R. Viswanathan (September 1984).
5. Martin, P. F., Kuhnen, G., and Graves, D., "Major Turbine Rotor Weld Repairs Utilizing Partial Forgings," Proceedings of Seminar on Life Assessment and Improvement of Turbo-Generator Rotors for Fossil Plants, Raleigh, North Carolina, EPRI CS-4160 (September 1984).
6. Clark, R. E., Schmerling, J. M., Kramer, L. D. and Amos, D. R., "Experiences with Weld Repair of Low Pressure Steam Turbine Rotors," American Power Conference, Chicago, Illinois (April 1985).
7. Kramer, L. D., Clark, R. E., Nottingham, L. D., Rust, T. M. and Swaminathan, V. P., "Life Extension Technique for Large Steam Turbine Rotors", Proceedings of Seminar on Life Assessment and Improvement of Turbo-Generator Rotors for Fossil Plants, Raleigh, North Carolina, EPRI CS-4160 (September 1984).
8. Viswanathan, R., "Emerging Nondestructive Techniques for Damage Assessment," Proceedings of International Conference on Advances in Material Technology for Fossil Power Plants, Chicago, Illinois (September 1987).
9. Stout, R. D. and Doty, W. D., Weldability of Steels, Second Edition, New York, New York: Welding Research Council (1971).

10. Welding Handbook, 7th Ed., 4, American Welding Society, Miami, Florida (1982).

11. Pellini, W. S. and Puzak, P. P., "Fracture Analysis Diagram Procedures for Fracture-Safe Engineering Design in Steel Structures," WRC Bulletin 88, Welding Research Council, New York, New York (May 1963).

12. Barsom, J. M. and Rolfe, S. T., Fracture and Fatigue Control in Structures, Second Edition, Englewood, New Jersey: Prentice-Hall, Incorporated, (ISBN 0-13-329863-9) (1987).

13. Barsom, J. M. and Rolfe, S. T., "Correlations Between KIc and Charpy V-Notch Test Results in the Transition-Temperature Range," Impact Testing of Metals, ASTM STP 466, ASTM, pp. 281-302 (1970).

14. Rolfe, S. T. and Novak, S. R., " Slow-Bend KIc Testing of Medium-Strength High-Toughness Steels," Review of Developments in Plain Strain Fracture Toughness Testing, ASTM STP 463, ASTM, pp.124-159 (1970).

15. Paris, P. C., "The Growth of Cracks Due to Variations in Load," Ph.D. Dissertation, Lehigh University (1962).

16. Imhoff, E. J., Barsom, J. M., "Fatigue and Corrosion— Fatigue Crack Growth of 4340 Steel at Various Yield Strengths," ASTM STP 536 (1973).

17. Forman, R. G., Kearney, V. E., and Engle, R. M., "Numerical Analysis of Crack Propagation in Cyclic Loaded Structure," Journal of Basic Engineering, 89D (1969).

18. Clarke, G. A., Shin, T. T., and Kramer, L. D., "Steam Turbine Rotor Reliability–Task Details, Task 4 Material Mechanical Properties Measurement," EPRI NP-923, Project 502 Interim Reports (November 1978).

19. Collipriest, J. E. and Ehret, R. M., "A Generalist's Relationship Representing the Sigmoidal Distribution of Fatigue-Crack-Growth Rates," Rockwell International Report SD-74-CE-0001 (1974).

20. Fatigue Crack Growth Computer Program "NASA/FLAGRO," Users' Manual, JSC-22267, NASA Lyndon B. Johnson Space Center (March 1989).

21. Brockenbrough, R. L. and Johnston, B. G., Steel Design Manual, United States Steel Corporation, ADUSS 27-3400-04 (January 1981).

22. Clark, W. G., Jr., "Fatigue Crack Growth Characteristics of Heavy Section ASTM A533 Grade B Class 1 Steel Weldments," ASME Paper 70-PVP-24 (1970).

23. Amos, D. R. and Clark, R. E., "Narrow Groove Welding of Steam Turbine Rotors," Proceedings from International Conference on Advances in Welding Science and Technology, Gatlinburg, Tennessee, Ed: S. A. David; Publ: ASM International, Metals Park, Ohio, pp. 315-323. (ISBN 0-87170-245-2) (May 1986).

24. Welding Handbook, 8th Ed., 2, American Welding Society, Miami, Florida (1991).

25. Dowson, P., "Submerged Arc Welding for Restoration of Ashland Axial Rotor," United Technologies Elliott Technical Report No. 370, Unpublished (May 1986).

26. Fuentes, K. and Hodas, L. J., "Rotating Beam Fatigue Testing– Weld Repaired Shaft from Elliott Company," Unpublished Technical Memorandum, Radian Corporation, Austin, Texas (June 1986).

ACKNOWLEDGEMENTS

The mock up test assemblies produced for this study were the result of innovative welding techniques developed by Roy Peterson and precise nondestructive testing techniques developed by William Ribbing. The destructive and metallurgical testing and recording of data was provided by Douglas Richards, Frank Danowski, John Disantis, and Richard Wiegand, under the competent supervision of Phillip Dowson, Manager of Materials Engineering.